Journal of Engineering and Sustainable Development
https://jeasd.uomustansiriyah.edu.iq/index.php/jeasd
https://doi.org/10.31272/jeasd.28.3.6

Vol. 28, No. 03, May 2024
ISSN 2520-0917

Original Research

FUZZY MAXIMUM POWER POINT TRACKING CONTROLLERS FOR PHOTOVOLTAIC SYSTEMS: A COMPARATIVE ANALYSIS

Ammar Al-Gizi[1*], Abbas Hussien Miry[2], Hussein M. Hathal[3], Aurelian Craciunescu[4]

[1,2,3]*Electrical Engineering Department, College of Engineering, Mustansiriyah University, Baghdad, Iraq*
[4]*Electrical Engineering Faculty, University Politehnica of Bucharest, Bucharest, Romania*
[1]https://orcid.org/0000-0002-4200-665X
[2]https://orcid.org/0000-0002-7456-287X
[3]https://orcid.org/0000-0002-3670-5585

Received 22/08/2023 ***Revised 14/04/2024*** ***Accepted 20/04/2024***

Abstract: The design of an effective fuzzy maximum power point tracking controller plays a crucial aspect in enhancing the photovoltaic system's efficiency. This article aims to design and compare the performance of symmetric and asymmetric types of fuzzy controllers' maximum power point tracking algorithms. Depending on the BP SX150S module' power-voltage attributes at standard technical conditions, the input membership function parameters are derived. Moreover, the effect of fuzzy memberships' quantity is also examined in this article. Where Five and seven triangular memberships are used. For the simulation, MATLAB is used to assess the effectiveness of the fuzzy controllers. Simulation results show that the asymmetric controller outperforms the symmetric type in terms of transient and steady-state tracking for different numbers of membership functions. Specifically, when employed with 5-triangle memberships, the asymmetric controller outperforms the symmetrical controller in terms of rise time, tracking precision, and energy output, respectively, by 83%, 0.06%, and 14.14%. While, the rise time, tracking precision, and energy yield of 7-triangle memberships are all improved by 86.7%, 0.04%, and 14.78%, respectively. Using asymmetric type, 7-triangle memberships enhance the rise time and harvested energy by around 18.2% and 0.082%, respectively. Overall, the most effective tracking technique for enhancing the photovoltaic system's efficiency is the asymmetric type, independent of the quantity of memberships.

Keywords: *Energy Yield; Fuzzy Controllers; Maximum Power Point Tracking; Perturb and Observe; Photovoltaic.*

1. Introduction

In a photovoltaic (PV) system, the operational point at which a solar panel generates its greatest power output is called the maximum power point (MPP). The MPP changes with environmental factors like solar irradiance (G) and temperature (T) [1-4]. Since the current-voltage relationship is complicated and exponentially nonlinear, determining the photovoltaic module's MPP is challenging. Because the MPP location is unknown, many MPPT algorithms have been used to find it. The MPPT controller is utilized to continuously adjust the PV system's operating point to track the MPP and maximize the energy harvest through appropriate modification for the DC/DC converter's duty (D) [2]. Fuzzy logic (FL), incremental conductance (InC), and perturb and observe (P&O) algorithms are common PV MPPT techniques utilized for this objective [5, 6]. InC and P&O tracking techniques usually cause an energy loss due to a fluctuation around

*Corresponding Author:
ammar.ghalib@uomustansiriyah.edu.iq

the MPP [7, 8]. Currently, the fuzzy MPPT is a popular choice to locate and monitor the PV system's MPP because of its efficiency and ability to adapt to complicated systems. Where the PV system's detailed mathematical model is unnecessary when utilizing the FLC-based MPPT. Rather, it makes control decisions based on linguistic rules and expert knowledge. This simplifies implementation and eliminates the need for costly calculations [9]. PV systems with FLC MPPT can perform superior to PV systems that employ conventional P&O or InC tracking techniques in both transient and steady-state performances [10-14]. FLC with symmetric types of MFs outperforms the conventional P&O technique concerning tracking speed and precision, especially at varying and challenging environmental conditions [10, 11], [15-17]. The PV system's efficiency is improved by using a 5-tri MFs asymmetric controller [18, 19]. MFs' parameters are calculated by the power-voltage (*P*-*V*) curve's characteristic. The description of MFs and rules is a crucial part of the fuzzy controller structure. Trial and error are often used to establish MFs for traditional controllers, although this method does not provide the intended outcomes [20]. Because the setting values of MFs in an FLC-based MPPT system can greatly influence its effectiveness, researchers and practitioners often turn to various optimization techniques to automatically seek the best values for the MFs rather than a trial-and-error [21-23]. The asymmetric fuzzy controller with 5-tri MFs offers the greatest PV system's dynamic and stable tracking results when compared to the symmetric fuzzy controller and P&O-based MPPT approaches [19]. In this article, symmetric and asymmetric fuzzy controllers with 5 and 7 triangular MFs are proposed. To further demonstrate the improvements of the suggested fuzzy MPPT approaches, the conventional P&O established in [24] is also provided. Section 2 is dedicated to explaining the mathematical model of the PV system being used in the article; Section 3 describes the proposed symmetric and asymmetric types of FLCs-based MPPT. Meanwhile, Section 4 presents the outcomes of the simulations. Finally, Section 5 summarizes the key findings of the article.

2. Modeling of PV System

First, As shown in Fig. 1, the primary parts of a conventional stand-alone PV system are a module, load, and tracking system that includes a DC/DC converter and a tracking technique. The following elements are used in this article:

- BP SX150S module with (N_S=72) cells linked in series,
- DC/DC converter (ideal buck-boost type),
- Load of resistance (R_L=6Ω),
- MPPT techniques as fuzzy and P&O.

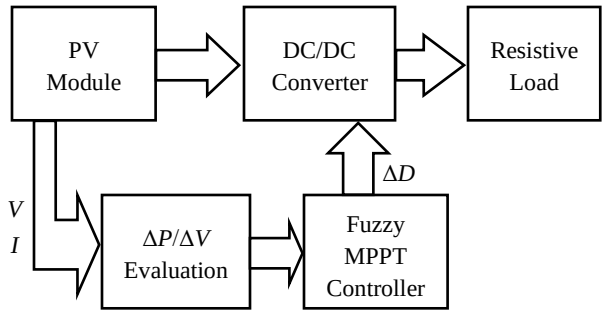

Figure 1. Conventional stand-alone PV system

Under STC, the BP SX150S module has the greatest output power of 150 W. At these conditions, the cell temperature T_r and solar irradiance G_r are 25 ^oC and 1000 W/m^2, respectively. Table 1 is a list of the electric specifications for the PV module in use [25].

Table 1. Specifications of BP SX150S module under

Parameter	Value
Maximum Power (P_{max})	150 W
Open-circuit voltage (V_{oc})	43.5 V
Short-circuit current (I_{sc})	4.75 A
Voltage at Pmax (V_{mpp})	34.5 V
Current at Pmax (I_{mpp})	4.35 A
Temperature coefficient of V_{oc}	−(160 ± 20) mV/ ºC
Temperature coefficient of I_{sc} (α)	(0.065 ± 0.015) %/ ºC
Temperature coefficient of power	−(0.5 ± 0.05) %/ ºC

To identify the point of operation at MPP and draw the most power possible from the PV module, it is necessary to maintain the compatibility between the converter's input impedance (R_{in}) and the PV optimum impedance (R_{opt}) using a DC/DC converter [11] as expressed by:

$$R_{opt} = \frac{V_{mpp}}{I_{mpp}} \quad (1)$$

At the MPP, the module's voltage and current can be denoted as V_{mpp} and I_{mpp}, respectively.

The input impedance of an ideal DC/DC converter (as seen by the PV module) is:

$$R_{in} = \frac{V}{I} = \frac{V_L}{I_L} \times \frac{(1-D)^2}{D^2} = R_L \times \frac{(1-D)^2}{D^2} \quad (2)$$

The converter's duty cycle is denoted by D, while I_L and V_L are the load's current and voltage, respectively, and I and V are the module's current and voltage, respectively.

As expressed in (2), load matching can be satisfied by amending the value of D. By decreasing D, the operating point moves clockwise (i.e., the module voltage increases) and vice versa. By a single-diode PV cell, the operational point of a module defined by its current and voltage at various G and T is expressed by:

$$I = I_{ph} - I_o\left(exp\left(\frac{q(V+IR_s)}{N_s nKT}\right) - 1\right) - \left(\frac{V+IR_s}{R_{sh}}\right) \quad (3)$$

I-V equation as a function of R_{in} is:

$$V - R_{in}I = V - R_{in}f(V,G,T) = 0 \quad (4)$$

I_{ph} denotes a light current and I_{sc} denotes a short-circuit current. I_o is a cell's reverse current, K is Boltzmann's constant, q is an electron charge, and n is an ideality factor of the diode (often symbolized by "A"), whose value ranges between 1 and 2 (1.62 in this article) and is used to modify the module's *I-V* characteristics into their actual characteristics [26].

The reverse saturation current (I_o) is temperature dependent and is expressed as:

$$I_o = I_{or} \times \left(\frac{T}{T_r}\right)^3 \times exp\left(\frac{qE_g}{nK}\left(\frac{1}{T_r} - \frac{1}{T}\right)\right) \quad (5)$$

E_g is a cell's semiconductor band gap energy.

However, the PV module short-circuit current (I_{sc}) as follows:

$$I_{sc} = \frac{G}{G_r}\left(I_{scr} + \alpha(T - T_r)\right) \quad (6)$$

By varying a parameter D from 0 to 1 with a step of 0.05 and by using the Newton-Raphson method to solve nonlinear equations (2), (3), and (4), the plots of voltage change (ΔV), power change (ΔP), and the power $\Delta P/\Delta V$ relationship can be found. These plots are depicted in Figs. 2, 3, and 4, respectively, at various G and a fixed T of 25 ºC.

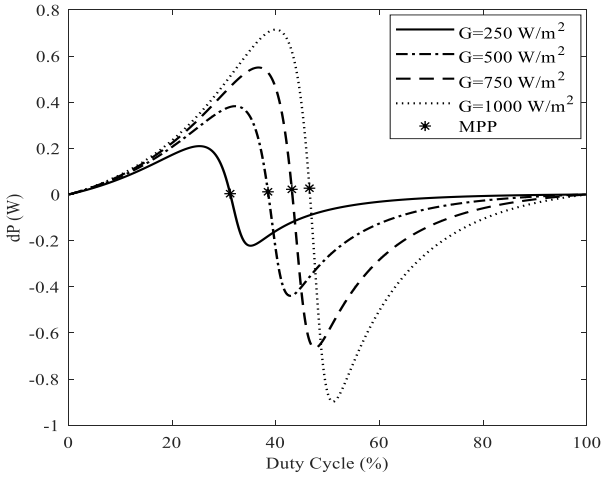

Figure 2. PV module's d*P* curves at varying *G* and a fixed *T* of 25 ºC

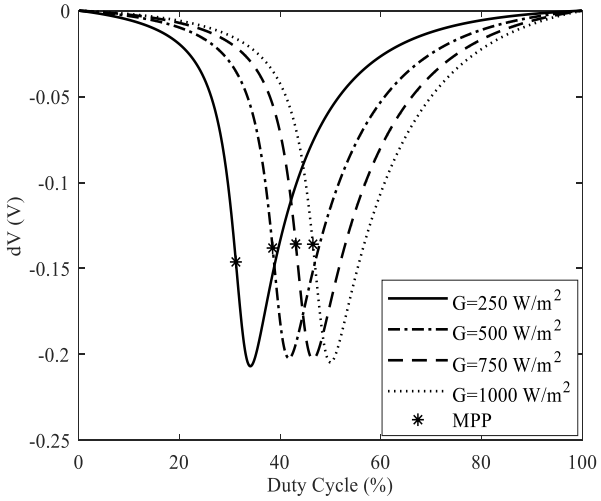

Figure 3. PV module's d*V* curves at varying *G* and a fixed *T* of 25 ºC

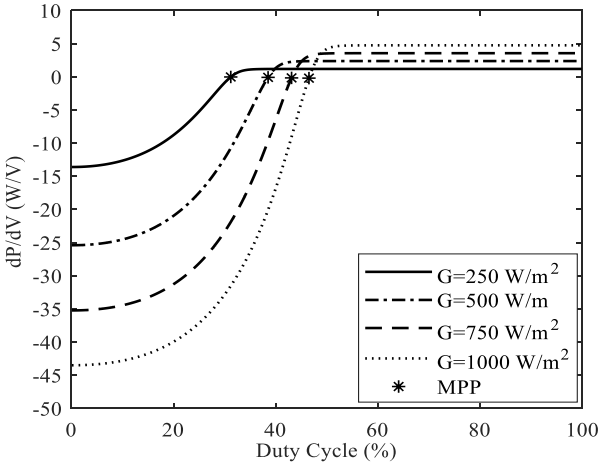

Figure 4. PV module's d*P*/d*V* curves at varying *G* and a fixed *T* of 25 ºC

3. Fuzzy MPPT Controller

The MPPT control algorithm is used to determine the optimal value of *D*. Fuzzy logic is a control system methodology that uses linguistic variables and rules to approximate human reasoning. FLCs are effective in handling non-linear and uncertain systems, making them suitable for MPPT in PV systems, where environmental conditions can vary [9]. To preserve the MPP, the fuzzy MPPT modifies the DC/DC converter's duty. Fig. 5 depicts the FLC structure.

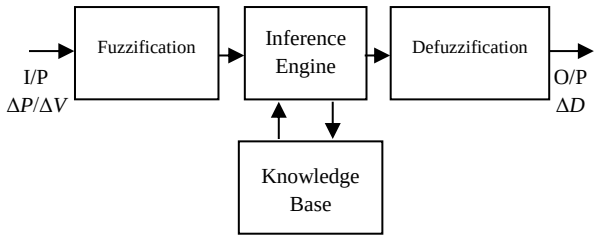

Figure 5. The FLC structure

The power variation (Δ*P*/Δ*V*) and duty variation (Δ*D*) serve as the controller's input and output that are suggested in this article. Meanwhile, the linguistic symbols: negative (*NE*), zero (*ZE*), and positive (*PO*) are employed to indicate the input and output of the controller.

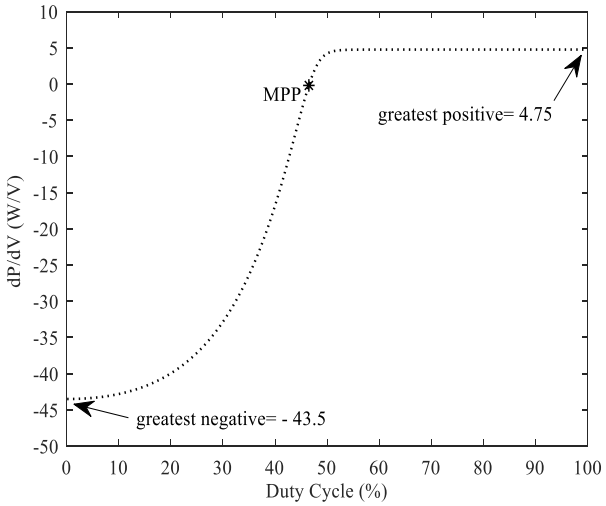

Figure 6. PV module's d*P*/d*V* curve at STC

By looking at the Δ*P*/Δ*V* curve illustrated in Fig. 6, the control rules are simply demonstrated.

Table 2 demonstrates that the FLC with five MFs has five rules in its rule base (RB) [26-29]. However, in the event of 7-MFs, the rules will be 7, as indicated in Table 3 [26]. The operational point's proximity to the MPP determines the rules. *D* will be gently raised or lowered to locate the MPP if the point of operation gets close to it, and conversely.

Table 2. Rules of a 5-MFs FLC [26]

dP/dV	*NEB*	*NES*	*ZE*	*POS*	*POB*
Δ*D*	*POB*	*POS*	*ZE*	*NES*	*NEB*

Table 3. Rules of a 7-MFs FLC [26]

dP/dV	*NEB*	*NEM*	*NES*	*ZE*	*POS*	*POM*	*POB*
Δ*D*	*POB*	*POM*	*POS*	*ZE*	*NES*	*NEM*	*NEB*

The center of gravity approach is utilized to obtain Δ*D* crisp value, as shown in Fig. 5 during a defuzzification stage as:

$$\Delta D = \frac{\sum_{i=1}^{n} \Delta D_i \times \mu(\Delta D_i)}{\sum_{i=1}^{n} \mu(\Delta D_i)} \quad (7)$$

At rule, *i*, μ(ΔD_i) and ΔD_i represent the fuzzy and crisp values of the output, respectively. *n* is the rules' quantity (5 when there are only five rules and 7 when there are only seven rules). In contrast, Δ*D* is the FLC output's final crisp value. As a result, the actual value of the duty cycle can be calculated depending on the produced Δ*D* [11]. The parameters of the MFs have an impact on the efficiency of the fuzzy MPPT [21]. In this article, symmetric and asymmetric FLCs are used, employing 5 and 7 triangular MFs in each type.

3.1. Symmetric FLC

The input of the symmetric controller is depicted in Fig. 7, utilizing 5-MFs and 7-MFs. The greatest positive and negative Δ*P*/Δ*V* readings are -43.5 and 43.5, respectively.

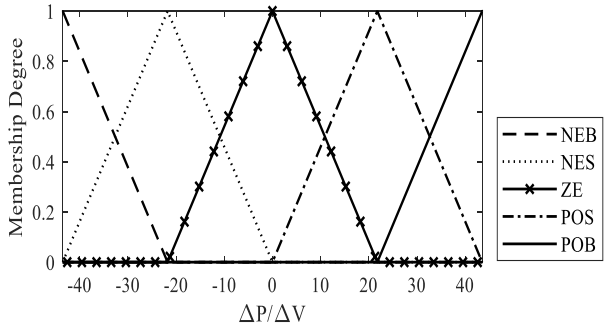

(a)

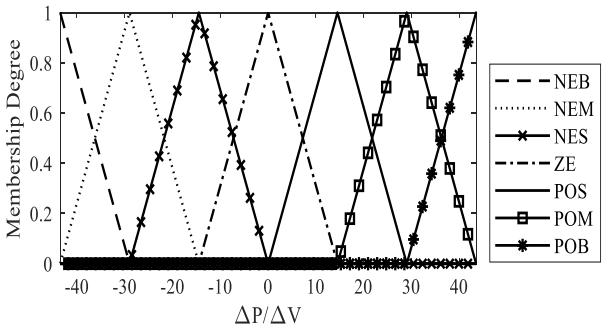

(b)

Figure 7. Symmetric controller's input: (a) 5-MFs; (b) 7-MFs

A large value of FLC output (Δ*D*) enhances the transient reaction expressed by the tracking speed but increases the steady-state ripple, and conversely. In this work, the greatest positive and negative Δ*D* are fixed at 0.05 and -0.05, respectively. The membership functions of Δ*D* for the symmetric type are shown in Fig. 8.

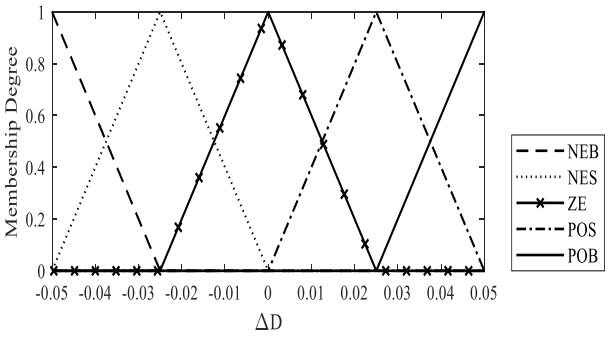

(a)

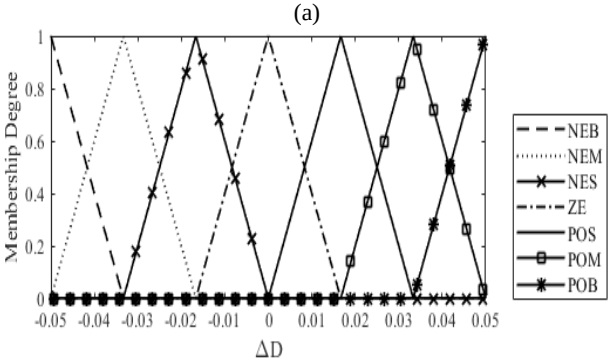

(b)

Figure 8. Symmetric controller's output: (a) 5-MFs; (b) 7-MFs

3.2. Asymmetric FLC

At STC, Fig. 6 shows that the values of Δ*P*/Δ*V* around MPP are asymmetric. Its value on the left side of MPP is smaller than the value on the

right. Hence, it is straightforward to design an asymmetric MF for FLC based on this characteristic.

From Fig. 6, by using the same Δ*D*, the greatest positive Δ*P*/Δ*V* (right side of MPP) is 4.75, whereas a negative reading of Δ*P*/Δ*V* is -43.5 (left side of MPP). As a result, and according to the symmetric MFs of Δ*D* illustrated in Fig. 8, the magnitude of the greatest negative reading of Δ*P*/Δ*V*, *NEB* has to be 43.5/4.75 times the greatest positive reading, *POB*. Hence, the greatest positive and negative readings of Δ*P*/Δ*V* are set as 4.75 and -43.5, respectively.

The asymmetric controller's input using 5-MFs and 7-MFs is depicted in Fig. 9.

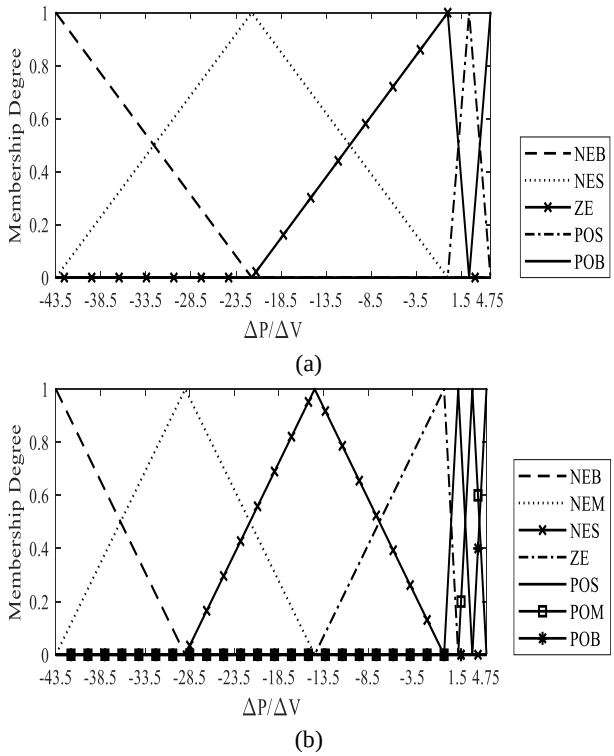

Figure 9. Asymmetric controller's input: (a) 5-MFs; (b) 7-MFs

4. Results and Discussions

Under STC and over 30s, the simulation results using P&O, symmetric, and asymmetric fuzzy tracking algorithms are analyzed. The starting point of operation is selected on the MPP's left side, assuming a starting duty of 0.9. The article analyzes and compares the results of various tracking algorithms using three metrics: steady state precision, energy output, and rise time t_r. The definitions of these metrics are outlined as:

$$\text{Precision (\%)} = \frac{P_{av}}{P_{MPP}} \times 100 = \frac{\int_{t_r}^{t_f} V \cdot I \; dt}{\int_{t_r}^{t_f} P_{MPP} \; dt} \times 100 \quad (8)$$

$$\text{Energy Output (Wh)} = \frac{\int_0^{t_f} P(t) \; dt}{3600} \quad (9)$$

P_{av} represents the steady-state average power, P_{MPP} represents the MPP's greatest power, $P(t)$ represents a current power at the moment t, t_f refers to a total simulation duration, and t_r represents the amount of time needed for the generated power to go up from 0.10 to 0.90 of its ultimate value [30]. The generated power from the PV module applying various MPPT algorithms is displayed in Fig. 10, employing 5-MFs. Fig. 11 depicts the output power using seven MFs.

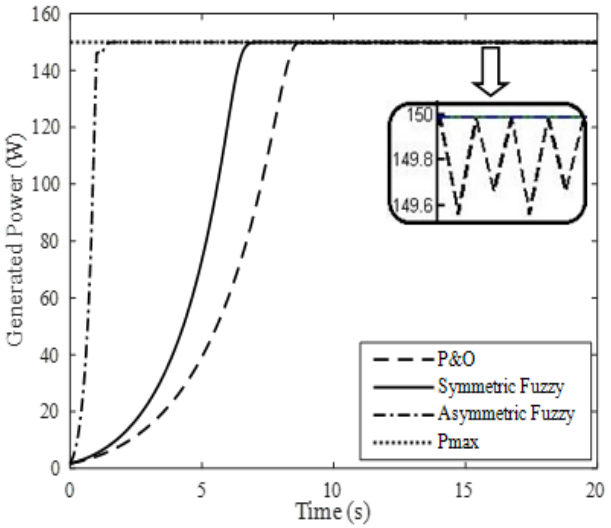

Figure 10. Generated power applying MPPT algorithms using 5-MFs at STC

Furthermore, Table 4 examines the effectiveness of the three MPPT algorithms. With regard to transient and steady-state performances, Fig. 10 and Fig. 11 illustrate that the symmetric fuzzy tracking algorithm surpasses the conventional

P&O algorithm. Furthermore, with 5-MFs and 7-MFs, the asymmetric fuzzy tracking algorithm outperforms both P&O and symmetric fuzzy controller.

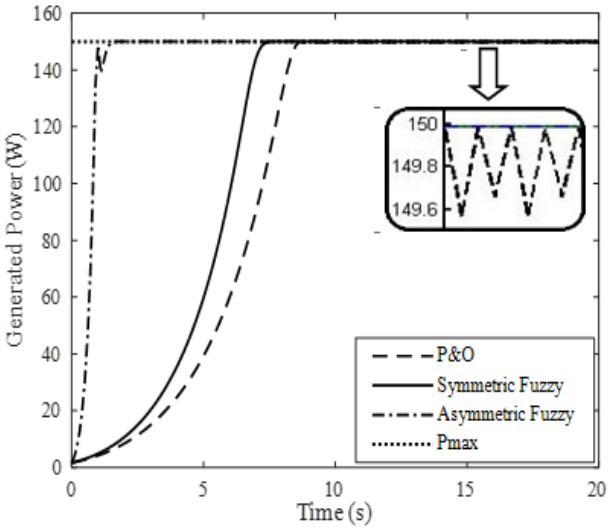

Figure 11. Generated power applying MPPT algorithms using 7-MFs at STC

Table 4. Effectiveness of tracking algorithms

Tracking Algorithms	Steady-State Power* (W)	Steady-State Precision (%)	Rise Time (s)	Energy Output** (Wh)
P&O (ΔD=0.005)	149.64	99.77	8.1	1.0
Symmetric (5-MFs)	149.87	99.91	6.4	1.05
Asymmetric (5-MFs)	149.94	99.97	1.1	1.223
Symmetric (7-MFs)	149.84	99.90	6.8	1.043
Asymmetric (7-MFs)	149.90	99.94	0.9	1.224

* MPP's ideal power is 149.988 W.
** Ideal energy output is 1.25 Wh.

With a 5-MFs asymmetric fuzzy controller, the module can produce energy of 1.223 Wh by locating the MPP with t_r of 1.1 s and a precision of 99.97%. t_r, precision and energy output are 6.4 s, 99.91%, and 1.05 Wh, respectively, when utilizing a symmetric fuzzy controller, as illustrated in Fig. 10 and Table 4. In comparison, an asymmetric fuzzy controller of 7-MFs can achieve the MPP with 0.9 s and a precision of 99.94%. As a result, the PV module can produce 1.224 Wh of energy. While employing a symmetric fuzzy controller, t_r, precision, and energy output are 6.8 s, 99.9%, and 1.043 Wh, correspondingly, as illustrated in Fig. 11 and Table 4. Similarly, the asymmetric fuzzy controller of 7-MFs surpasses that type of 5-MFs concerning rise time and energy output. Where, with an asymmetric fuzzy controller of 5-MFs and 7-MFs, t_r is 1.1 s and 0.9 s, respectively. Table 4 illustrates that the maximum energies collected from the module utilizing an asymmetric fuzzy controller of 5-MFs and 7-MFs are 1.223 Wh and 1.224 Wh, respectively. Moreover, Table A-1 in Appendix A illustrates a comparative result with other relevant research presented in the literature.

5. Conclusions

This article proposes symmetric and asymmetric types of fuzzy tracking algorithms utilizing triangular 5-MFs and 7-MFs. Depending on three metrics, namely precision, rise time, and energy output, the effectiveness of tracking algorithms is assessed and compared to the standard P&O at STC, allowing the most efficient MPPT algorithm to be discovered. When compared to other MPPT methods, the asymmetric fuzzy tracking algorithm with 5-MFs and 7-MFs produces better results. It has the best precision, energy output, and lowest t_r, as illustrated in Fig. 10, Fig. 11, and Table 4. Further, with regard to rise time and energy output, the asymmetric fuzzy tracking algorithm of 7-MFs outperforms the tracking algorithm of 5-MFs. Table 4 shows that rise time and energy output have been enhanced by 18.2% and 0.08%, respectively. Overall, and irrespective of

the quantity of MFs, the most promising MPPT strategy for enhancing overall PV system performance is the asymmetric FLC.

Acknowledgments

The authors would like to express their appreciation to Mustansiriyah University (www.uomustansiriyah.edu.iq), Baghdad-Iraq for its assistance and academic advice in the writing of this work.

Conflict of Interest

The authors declare that there are no conflicts of interest regarding the publication of this article.

Author Contributions Statement

Authors: Ammar Al-Gizi and Abbas H. Miry proposed the research problem.

Authors: Ammar Al-Gizi and Hussein M. Hathal developed the theory and carried out the calculations.

Authors: Ammar Al-Gizi, and Aurelian Craciunescu verified the analytical methods and investigated the performance comparisons of symmetric and asymmetric fuzzy MPPT controllers' algorithms and managed the results of this article.

All authors analyzed the findings and participated in the final article.

References

1. Belu, R., (2019). *Fundamentals and Source Characteristics of Renewable Energy Systems Photovoltaics*. 2019, United States: CRC Press. ISBN: 9781000448887.
2. Mustafa, R. J., Gomaa, M. R., Al-Dhaifallah, M., & Rezk, H, (2020). *Environmental impacts on the performance of solar photovoltaic systems*. Sustainability, Vol. 12, No. 2. https://doi.org/10.3390/su12020608.
3. Ali, R., Obaid, A.J., and Rasheed, H., (2020). *Performance analysis of photovoltaic cells at varying environmental parameters and solar cell precise algorithm*. in Journal of Physics: Conference Series - Imam Al-Kadhum International Conference for Modern Applications of Information and Communication Technology, MAICT 2019. Baghdad, Iraq: Institute of Physics Publishing. http://doi.org/10.1088/1742-6596/1530/1/012156.
4. Hasan, K., Yousuf, S. B., Tushar, M. S. H. K., Das, B. K., Das, P., & Islam, M. S . (2022). *Effects of different environmental and operational factors on the PV performance: A comprehensive review*. Energy Science and & Engineering, Vol. 10, No. 2, pp. 656-675. https://doi.org/10.1002/ese3.1043.
5. Podder, A.K., Roy, N.K., and Pota, H.R., (2019). *MPPT methods for solar PV systems: a critical review based on tracking nature*. IET Renewable Power Generation, Vol. 13, No. 10, pp. 1615-1632. https://doi.org/10.1049/iet-rpg.2018.5946
6. Lagdani, O., Trihi, M., and Bossoufi, B., (2019). *PV array connected to the grid with the implementation of MPPT algorithms (INC, P&O, and FL Method)*. Int. J. Power Electron. Drive Syst., Vol. 10, No. 4, pp. 2084-2095. http://doi.org/10.11591/ijpeds.v10.i4.pp2084-2095.
7. Motahhir, S., El Hammoumi, A., El Ghzizal, A., (2018). *Photovoltaic system with quantitative comparative between an improved MPPT and existing INC and*

P&O methods under fast varying of solar irradiation. Energy Reports, Vol. 4, pp. 341 - 350.

https://doi.org/10.1016/j.egyr.2018.04.003.

8. Abo-Sennah, M.A., El-Dabah, M.A., and Mansour, A., (2021). *Maximum power point tracking techniques for photovoltaic systems: a comparative study*. Int. J. Electr. Comput. Eng., Vol. 11, No. 1, pp. 57-73. http://doi.org/10.11591/ijece.v11i1.pp57-73.
9. Duair, J.J., Majeed, A.I., and Ali, G.M., (2021). *Design of maximum power point tracker controller for boost converter photovoltaic array system based on fuzzy Mamdani logic*. Journal of Engineering and Sustainable Development (JEASD), Vol. 25, No. Special, pp. 1-13-1-25. https://doi.org/10.31272/jeasd.conf.2.1.3.
10. Singh, J., Singh, S. P., Verma, K. S., & Kumar, B. (2022). *Comparative analysis of MPPT control techniques to enhance solar energy utilization and convergence time under varying meteorological conditions and loads*. Front. Energy Res., Vol. 10, 856702. https://doi.org/10.3389/fenrg.2022.856702.
11. Saber, H., Rahmani, L., & Radjeai, H. (2022). *A comparative study of the FLC, INC, and P&O methods of the MPPT algorithm for a PV system*. in 2022 19th International Multi-Conference on Systems, Signals & Devices (SSD). Setif, Algeria. https://doi.org/10.1109/SSD54932.2022.9955905.
12. Dehghani, M., Taghipour, M., Gharehpetian, G. B., & Abedi, M. (2020). *Optimized fuzzy controller for MPPT of grid-connected PV systems in rapidly changing atmospheric conditions*. Journal of Modern Power Systems and Clean Energy, Vol. 9, No. 2, pp. 376-383. https://doi.org/10.35833/MPCE.2019.000086.
13. Devarakonda, A. K., Karuppiah, N., Selvaraj, T., Balachandran, P. K., Shanmugasundaram, R., & Senjyu, T. (2022). *A Comparative Analysis of Maximum Power Point Techniques for Solar Photovoltaic Systems*. Energies, Vol. 15, No. 22, pp. 1-30. https://doi.org/10.3390/en15228776.
14. Ahmed, R.H., Rhaif, S.H., and Hashem, S.A., (2023). *Fuzzy logic control to process change irradiation and temperature in the solar cell by controlling for maximum power point*. Journal of Engineering and Sustainable Development (JEASD), Vol. 27, No. 1, pp. 28-36. https://doi.org/10.31272/jeasd.27.1.3.
15. Kandemir, E., Cetin, N.S., and Borekci, S., (2017). *A comparison of perturb & observe and fuzzy-logic based MPPT methods for uniform environment conditions*. Period. Eng. Nat. Sci., Vol. 5, No. 1, pp. 16-23.
16. Chaibi, Y., Allouhi, A., Salhi, M., & El-Jouni, A. (2019). *Annual performance analysis of different maximum power point tracking techniques used in photovoltaic systems*. Prot. Control Mod. Power Syst., Vol. 4, 15. https://doi.org/10.1186/s41601-019-0129-1.
17. Louarem, S., Kebbab, F. Z., Salhi, H., & Nouri, H. (2022). *A comparative study of maximum power point tracking techniques for a photovoltaic grid-connected system*. Electrical Engineering & Electromechanics, No. 4, pp. 27-33.

https://doi.org/10.20998/2074-272X.2022.4.04

18. Verma, P., Garg, R., and Mahajan, P., (2020). *Asymmetrical fuzzy logic control-based MPPT algorithm for stand-alone photovoltaic systems under partially shaded conditions*. Scientia Iranica, Vol. 27, No. 6, pp. 3162-3174. https://doi.org/10.24200/sci.2019.51737.2338.

19. Verma, P., Garg, R., and Mahajan, P., (2020). *Asymmetrical interval type-2 fuzzy logic control based MPPT tuning for PV system under partial shading condition*. ISA Transactions, Vol. 100, pp. 251-263. https://doi.org/10.1016/j.isatra.2020.01.009.

20. Rai , R.K. and Rahi , O.P.(2022). *Fuzzy logic-based control technique using MPPT for solar PV system*. in *2022 First International Conference on Electrical, Electronics, Information and Communication Technologies (ICEEICT)*. Trichy, India. https://doi.org/10.1109/ICEEICT53079.2022.9768650.

21. Faisal, M., Hannan, M. A., Ker, P. J., Rahman, M. A., Begum, R. A., & Mahlia, T. M. I (2020). *Particle swarm optimized fuzzy controller for charging–discharging and scheduling of battery energy storage system in MG applications*. Energy Reports, Vol. 4, Supplement 7, pp. 215-228. https://doi.org/10.1016/j.egyr.2020.12.007.

22. Guo, L., and Abdul, N.M.M., (2021). *Design and evaluation of fuzzy adaptive particle swarm optimization based maximum power point tracking on photovoltaic system under partial shading conditions*. Front. Energy Res., Vol. 9, 712175. https://doi.org/10.3389/fenrg.2021.7121 75.

23. Al-Gizi, A., Miry, A.H., and Shehab, M.A., (2022). *Optimization of fuzzy photovoltaic maximum power point tracking controller using chimp algorithm*. Int. J. Electr. Comput. Eng., Vol. 12, No. 5, pp. 4549-4558. http://doi.org/10.11591/ijece.v12i5.pp4549-4558.

24. Mohamed, S.A., and Abd El Sattar, M., (2019). *A comparison study of P&O and INC maximum power point tracking techniques for grid-connected PV systems*. SN Appl. Sci. Techn.- Electrotechn. et Energ., Vol. 1, No. 2. https://doi.org/10.1007/s42452-018-0134-4.

25. Al-Gizi, A., Craciunescu, A., and Al-Chlaihawi, S., (2017). *Improving the performance of PV system using genetically-tuned FLC based MPPT*. In 2017 International Conference on Optimization of Electrical and Electronic Equipment (OPTIM) & 2017 Intl Aegean Conference on Electrical Machines and Power Electronics (ACEMP). Brasov, Romania: IEEE. https://doi.org/10.1109/OPTIM.2017.7975041.

26. Al-Gizi, A., Al-Chlaihawi, S., Louzazni, M., & Craciunescu, A. (2017). *Genetically optimization of an asymmetrical fuzzy logic based photovoltaic maximum power point tracking controller*. Adv. Electr. Comput. Eng., Vol. 17, No. 4, pp. 69–76. https://doi.org/10.4316/aece.2017.04009

27. Sutikno, T., Subrata, A.C., and Elkhateb, A., (2021). *Evaluation of Fuzzy Membership Function Effects for Maximum Power Point Tracking Technique of Photovoltaic System*.

IEEE Access, Vol. 9, pp. 109157-109165. https://doi.org/10.1109/ACCESS.2021.3102050.

28. Zand, S. J., Mobayen, S., Gul, H. Z., Molashahi, H., Nasiri, M., & Fekih, A. (2022). *Optimized Fuzzy Controller Based on Cuckoo Optimization Algorithm for Maximum Power-Point Tracking of Photovoltaic Systems*. IEEE Access, Vol. 10, pp. 71699-71716. https://doi.org/10.1109/ACCESS.2022.3184815.

29. Hameed, W. I., Saleh, A. L., Sawadi, B. A., Al-Yasir, Y. I., & Abd-Alhameed, R. A. (2019). *Maximum power point tracking for photovoltaic system by using fuzzy neural network*. Inventions, Vol. 4, No. 33, pp. 1-12. https://doi.org/10.3390/inventions4030033.

30. Mohamed, M.A.E., Nasser, A.S., and Eladly, M.M., (2023). *Arithmetic optimization algorithm based maximum power point tracking for grid-connected photovoltaic system*. Sci. Rep., Vol. 13, 5961. https://doi.org/10.1038/s41598-023-32793-0.

Appendix – A

In this section, Table A-1 summarizes a comparative result with other relevant research presented in the literature.

Table A-1. Comparative results with other relevant research

Reference	FLC i/p Variable Selection	Type of FLC I/O MFs	Design of FLC i/p MF	Rise Time t_r (s)	Output Power (W)
Current article	$\Delta P/\Delta V$ decrease computation complexity, avoid numerical inaccuracy, suitable for cost sensitive systems	5 and 7 triangular- MFs	Symmetric, Asymmetric (MF setting values are set based on the P-V curve under STC)	1.1 (Asymmetric 5-MFs) 0.9 (Asymmetric 7-MFs)	149.94 (Asymmetric 5-MFs) 149.90 (Asymmetric 7-MFs)
Ref. [25]	$E=\Delta P/\Delta V$, ΔE increase computation complexity, increase numerical inaccuracy	5 triangular-MFs only	Symmetric, MF setting values optimized by GA	4.16 (symmetric) 2.16 (optimized)	---
Ref. [23]	$\Delta P/\Delta V$ decrease computation complexity, avoid numerical inaccuracy, suitable for cost sensitive systems	7 triangular-MFs only	MF setting values optimized by the chimp algorithm	2.1	---
Ref. [29]	Irradiance G, Temperature T Not suitable for cost sensitive systems	3 bell-MFs for Fuzzy Neural Network (FNN)	MF setting values optimized by FNN	---	141